

INVESTIGATIONS ON PHYSICAL PROPERTIES OF Zn FERRITE NANOPARTICLES USING SOL-GEL AUTO COMBUSTION TECHNIQUE

P. SIVAKUMAR^{a,*}, K. THYAGARAJAN^b, A. G. KUMAR^c

^aResearch Scholar, JNTUA, Anantapuramu, A.P. 515002, India

^bDept. of Physics, JNTUA College of Engineering, Pulivendula, A.P.-516390, India

^cCollege of Physics and Energy, Shenzhen University, Shenzhen-518060, P.R. China

Nano crystalline Zn-ferrites have been synthesized by sol-gel auto combustion method using citric acid as fuel agent at different sintering temperatures (400 °C, 500 °C, 600 °C and 700 °C). The physical properties of nano Zn-ferrite was investigated using XRD, SEM, FTIR and TGA/DTA for structural, surface morphological, and thermal properties respectively. The single-phase cubic spinel structure of all the samples has been confirmed from X-ray diffraction analysis. Surface morphology studies reveal that the grains are clear with well defined grain boundaries and also found that the average grain size is maximum at 700 °C calcination temperature. FTIR spectra gives the confirm the phase of material at frequency bands(542 and 437 cm⁻¹). TGA and DTA curves represents low weight loss found in the material and it is a stable material.

(Received August 18, 2018; Accepted November 24, 2018)

Keywords: Sol-gel auto combustion, XRD., FE-SEM, FTIR, TGA/DTA

1. Introduction

Nano materials are considered very attractive compared to their bulk counterpart, due to their advanced physical and chemical properties, due to the phenomenon called quantum confinement. Therefore, the synthesis of conventional materials as well as new materials at the nano scale is attracting the attention of scientists. More over, the experimental conditions play a very important role in determining the shape, size and purity and hence the drastic modifications of the properties. Spinal ferrites have been investigated for their usual electrical and magnetic properties as well as for various technological applications including Ferro fluids [1], high-density magnetic recording media [2], biomedicine [3] and radar absorbent materials [4]. Zinc ferrite, ZnFe₂O₄, is one of the most widely studied materials [5], because the high quality ZnFe₂O₄ nano structure has generated a lot of interest owing to their potential applications in gas sensing [6], magnetic behavior [7], electrical characteristics [8] and semiconductor photo catalysis [9]. The spinel ferrites can generally be described by the formula AB₂O₄, where A and B denote divalent and trivalent cations, respectively. Bulk Zinc ferrite is a normal spinel structure, all of the A (Zn²⁺) sites are tetrahedrally coordinated while the B(Fe³⁺) sites are octahedrally coordinated by oxygen atoms [10]. But recent investigations [11, 12] on Nano particles of zinc ferrite report the presence of ferrimagnetic ordering at room temperature. This change in magnetic ordering is due to the redistribution or inversion of cations between the tetrahedral and octahedral sites. The migration of Fe³⁺ ions to the tetrahedral sites results in net magnetization due to the A–O–B super exchange mechanism. Thus the properties exhibited by ZnFe₂O₄ are likely to change with the particle size and inversion of cations in the sites. The inversion parameter in turn is dependent on the route of synthesis. The sol–gel auto-combustion method is used here has many simple processing steps. It has the advantages such as using inexpensive precursors and reducing in consumption of external energy by usage of auto-combustion process. The synthesis also results in the formation of Nano-sized, homogeneous and highly reactive powder [13]. Sol–gel combustion process offers a

*Corresponding author: sivakumar.pendyala@gmail.com

molecular-level mixing of the precursors, which is capable of improving chemical homogeneity of the resulting powders to a significant extent. However, since this method makes use of the exothermicity of redox reaction, agglomeration commonly exists in the ceramic powders synthesized by sol-gel combustion method. Agglomeration is commonly divided into soft agglomeration and hard agglomeration according to the strength of attractive force between particles [14]. Several preparation conditions such as dilution, fuel/oxidant ratio, pH and temperature can have an impact on the formation of the ferrites and their properties [15].

In the present study, the effect of the annealing temperature on the rearrangement of cations in A and B sites, and hence the overall effects on physical properties of ZnFe₂O₄ nanoparticles have been investigated.

2. Experimental

Nano particles of ZnFe₂O₄ have been prepared by sol-gel auto combustion method. Analytical grade Zn(NO₃)₂·6H₂O and Fe(NO₃)₃·9H₂O are mixed with citric acid. The ratio of the nitrates to citric acid is 1:3. The slurry mixture is then dissolved in 250 ml of deionized water. Citric acid helps for the homogenous distribution and segregation of the metal ions. Small amount of ammonium hydroxide is added carefully to the solution to change the pH value to 7. The solution is then continuously stirred using a magnetic stirrer. Condensation reaction occurs between adjacent metal nitrates and molecules of citric acid and forms a polymer like network which then grows into colloidal dimensions known as sol. The resultant sol is poured in a silica crucible and heated at 135 °C under constant stirring to transform into xerogel or dried gel. Continuous heating leads to the formation of Nano powder of Zn-ferrite through a self-propagating combustion process. Finally, the powdered yield was divided into four parts and these four samples were kept for annealing at different temperatures of 673, 773, 873 and 973K for four hours and encoded as 400 °C, 500 °C, 600 °C and 700 °C respectively.

3. Results and discussion

3.1. Structural analysis

The X-ray Diffraction patterns of the ZnFe₂O₄ system for different calcinations temperatures (400 °C, 500 °C, 600 °C & 700 °C) shown in above Fig. 1 it is Observed that ZnFe₂O₄ matches well with the standard JCPDS cardNo.22-1012 of pure ZnFe₂O₄ phase. Furthermore for all the samples, there is no clear change in peak's position and the absence of additional peaks, indicates that all the prepared samples crystallize within a single-phase of cubic structure with Fd3m space group. The intensity of main diffraction peak of cubic spinel ferrite at the (311) plane was considered as a measure of its degree of good crystallinity[16]. The linear variation of the lattice constant (*a*) was found to increase from 8.368 Å to 8.372 Å with the calcination temperature up to 700 °C which follows the Vegard's law. A small increase in lattice constant can be explained on the basis of the ionic radii of the substituent ions. It is assumed that the replacement of smaller Fe²⁺ ions (0.64Å) with the larger Zn²⁺ ions (0.74Å) on the octahedral sites causes the unit cell to expand which results in the increase of lattice constant. This is consistent with previous work reported by Ateia. E.E. and Mohamed. A.T. [17]. To understand the crystallite size of ZnFe₂O₄ calcined at different temperatures and was calculated using Scherrer's equation [15]:

$$D = \frac{k\lambda}{\beta \cos\theta} \quad (1)$$

Where *k*=0.9 is Scherrer's constant, $\lambda = 1.5406 \text{ \AA}$ is the wavelength of the incident x-rays, β is the full width at half maximum (FWHM) of diffraction peak, and θ is the Bragg's angle of diffraction. The variation of FWHM and crystallite size with respect to the calcinations temperature is shown in Fig. 2. The crystallite size (*D*) varies from 23.36 to 40.36 nm. The observed variation in crystallite size of Zn²⁺ substituted Fe²⁺ supports the observed lattice constant variation results.

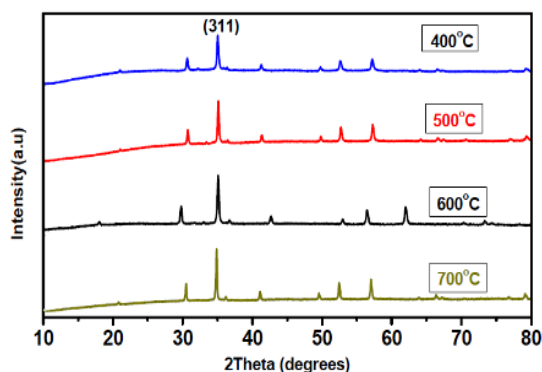


Fig. 1 XRD pattern for $ZnFe_2O_4$ Nano Particles.

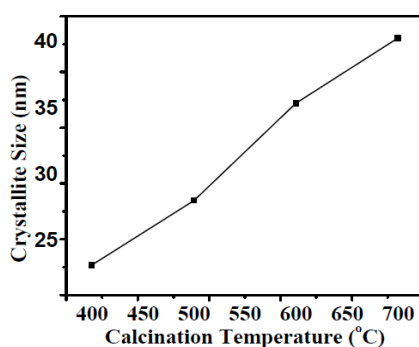


Fig. 2 Variation of crystallite size with Calcination temperature.

Table 1. Crystallite size and structure of the samples at different calcination temperatures

S.no	Temperature (°C)	2θ (°)	Crystallite size(nm)	structure
1	400	35.79	23.37	cubic
2	500	35.60	27.60	cubic
3	600	35.39	34.76	cubic
4	700	35.17	40.21	cubic

The SEM images of the Zn-ferrite samples (Fig. 3) show that the morphology of particles were almost spherical, regular in shape and dispersed uniformly, but agglomerated to some extent due to the interaction between the magnetic nanoparticles, whereas the gel exhibits a relatively porous network. The pressure exercised by gaseous species should be responsible for the breakup of the porous structure. Heat treatment resulted in agglomeration of the powder as a function of the calcining temperature which is typical for the spinel ferrites. Therefore, some degree of agglomeration at the higher calcination temperature appears unavoidable. In many cases of nanocrystalline ferrites, it is observed that there is a tendency of agglomeration among the nanoparticles [18].

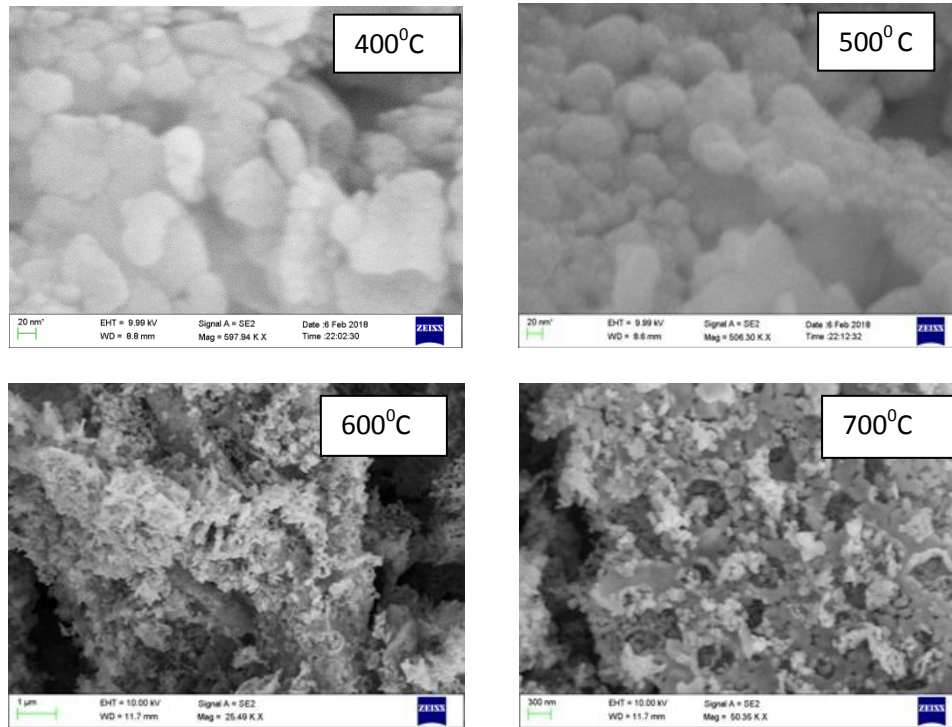


Fig. 3. SEM images of $ZnFe_2O_4$ at different calcination temperatures ($400^\circ C$, $500^\circ C$, $600^\circ C$ & $700^\circ C$ respectively).

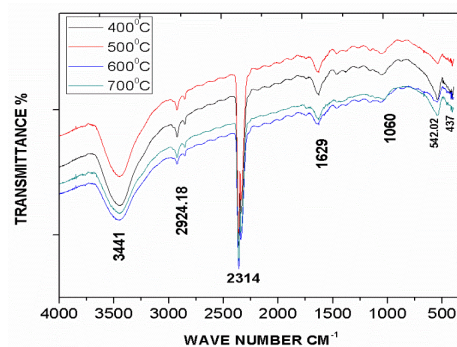


Fig. 4. FTIR spectra for different calcination temperatures of Zn ferrite.

FTIR spectra of Mg-ferrite nano particles calcined at different temperatures are shown in Fig. 4. For all samples, the bands observed at 542 and 437 cm^{-1} are attributed to tetrahedral and octahedral M-O (M=Fe and Zn) stretching vibration mode. The peaks at 3441, 2924, 1629 and 1060 cm^{-1} corresponds to metal-oxygen lattice vibrations [19], and also due to O-H stretching vibrational mode and H-O-H bending mode can be attributed to the presence of free water and hydroxyl group in the samples [20, 21]. when calcination temperature increases frequency of tetrahedral and octahedral absorption peaks are diminish in size due to cation redistribution. This is well accordance with Xrd result. The bands 542 and 437 represents' formation of single phase spinal structure.

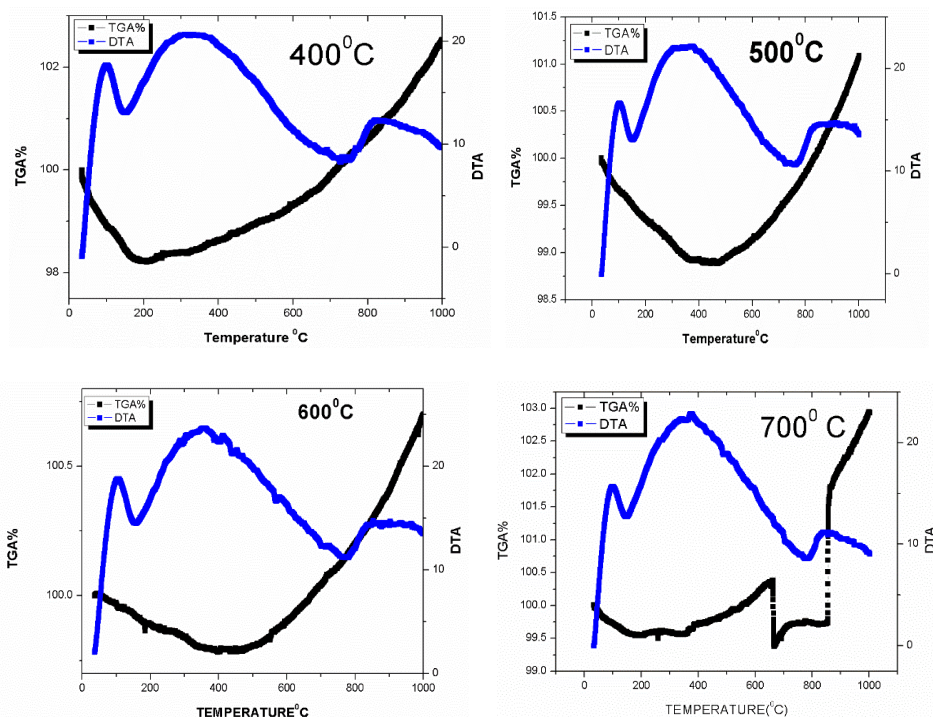


Fig. 5. Shows the TGA/DTA Curve for different calcination temperatures (400°C, 500°C, 600°C & 700°C).

3.2. Thermal analysis

From Fig. 5 the weight loss below 150 °C associated with an endothermic DTA peak arises from the loss of absorbed water. The first exothermic peak below 200°C in the DTA Curve, Accompanied by a very small weight loss 2% in TGA curve due to evolution of gases (such as CO, CO₂, NO₂ and water vapour) [22]. The Exothermic peaks at 400 °C and 825 °C represents formation of intermediate phases. Which are associated with the formation of Zn ferrite via solid state reaction. From above figures we concluded that the TGA curve decreases at low temperatures up to 400 °C and then increases linearly due to oxidation of Zn²⁺ to Zn³⁺ and Zn⁴⁺ [22]. When temperature increases loss in weight decreases at different endo thermic peaks. When temperature increase from 400 °C to 700 °C weight gain observed at 200 °C, 400 °C, 500 °C and 650 °C. Finally ZnFe₂O₄ is most stable material when temperature increases [23].

4. Conclusions

The Zinc ferrite Nano particles are successfully synthesized by sol-gel auto combustion technique. The XRD confirms the Zn Nano particles has cubic spinal structure. The crystallite size increases with increasing temperature (23.37 to 40.21 nm) which was also supported by FTIR and SEM analysis. From TGA and DTA curve When temperature increases loss in weight decreases at different endo thermic peaks. When temperature increase from 400 °C to 700 °C weight gain observed at 200 °C, 400 °C, 500 °C and 650 °C. Finally ZnFe₂O₄ is most stable material when temperature increases

References

- [1] K. Raj, R. Moskowitz, *Journal of Magnetism and Magnetic Materials* **85**, 233 (1990).
- [2] A. Moser, K. Takano, D. T. Margulies, M. Albrecht, Y. Sonobe, Y. Ikeda, S. Sun, E. E. *Journal of Physics D: Applied Physics* **35**, R157 (2002).
- [3] J. M. Bai, J. P. Wang, *Applied Physics Letters* **87**, 152502 (2005).
- [4] A.G.S. Kumar, L. Obulapathi, M. Maddaiah, T.S. Sarmash, D.J. Rani, J.V.V.N.K. Rao, T.S. Rao, and K. Asokan, *AIP Conference Proceedings* **1665**, 080002 (2015).
- [5] A. Montoya, N. Nava, A. Vázquez, *Applied Catalysis A* **198**, 235 (2000).

- [6] M. P. Pileni, *Advanced Functional Materials* **11**, 323 (2001).
- [7] J. F. Hocheplied, P. Bonville, M. P. Pileni, *Journal of Physical Chemistry B* **104**, 905(2000).
- [8] S. H. Yu, M. Yoshimura, *Chemistry of Materials* **12**, 3805 (2000).
- [9] A.G.S. Kumar, T.S. Sarmash, D.J. Rani, L. Obulapathi, G.V.V.B. Rao, T.S. Rao, K. Asokan, *Journal of Alloys and compounds*, **665**, 86–92 (2016)
- [10] M. N. Akhtar, N. Yahya, P. B. Hussain, *International Journal of Basic and Applied Sciences* **9**, 151 (2009).
- [11] C. N. Chinnasamy, A. Narayanasamy, N. Ponpandian, K. Chattopadhyay, H. Guerault, J. M. Grenèche, *Scripta Mater.* **44**, 1407 (2001).
- [12] S. D. Shenoy, P. A. Joy, M. R. Anantharaman, *J. Magn. Magn. Mater.* **269**, 217 (2004).
- [13] P. K. Roy, J. Bera, *Journal of Materials Processing Technology*, **197**, 279 (2008).
- [14] Q. Feng, X. H. Ma, Q. Z. Yan, C. C. Ge, *Materials Science and Engineering B* **162**, 53 (2009).
- [15] A.G.S. Kumar., T.S. Sarmash, L. Obulapathi, D.J. Rani, T.S. Rao, K. Asokan, *Thin Solid Films*, **605**, 102–107 (2016)
- [16] K.C.B. Naidu, T.S. Sarmash, M. Maddaiah, A.G.S. Kumar, D.J. Rani, V.S. Samyuktha, L. Obulapathi, T.S. Rao, *Journal of Ovonic Research*, **11(2)** 79 – 84, (2015).
- [17] E. E. Ateia, A. T. Mohamed, *J. Magn. Magn. Mater.* (2016).
- [18] M. Srivastava, S. Chaubey, K. O. Animesh, *Mater. Chem. Phy.* **118**, 174 (2009).
- [19] P. SivaKumar, K. Thyagarajan, A.G.S. Kumar, L. Obulapathi, *Journal of the Australian Ceramic Society*, **54**, 467–473(2018)
- [20] M. Maddaiah, A.G.S. Kumar, L. Obulapathi, T.S. Sarmash, K.C.B. Naidu, D.J. Rani, T.S. Rao, *Digest journal of nanomaterials and biostructures*, **10(1)** 155 – 159 (2015).
- [21] S. Moudar, M. Melnik, E. Jóna, *Thermochim. Acta* **352-353**, 127 (2000).
- [22] J. M. Yang, F. S. Yen, *Journal of Alloys and Compounds* **450**, 387 (2008).
- [23] J. Dantas, J. R. Santos, F. Silva, A. Silva, A. C. F. Costa, *Materials Science Forum* **775-776** , 705 (2014).